Influence of Solar Magnetic Sector Structure on Terrestrial Atmospheric Vorticity

JOHN M. WILCOX, PHILIP H. SCHERRER AND LEIF SVALGAARD
Institute for Plasma Research, Stanford University, Stanford, Calif. 94305

WALTER ORR ROBERTS
University Corporation for Atmospheric Research, Boulder, Colo. 80302

ROGER H. OLSON
Environmental Data Services, NOAA, Boulder, Colo. 80302

ROY L. JENNE
National Center for Atmospheric Research,[1] Boulder, Colo. 80302

(Manuscript received 13 July 1973)

ABSTRACT

The solar magnetic sector structure has a sizable and reproducible influence on tropospheric and lower stratospheric vorticity. The average vorticity during winter in the Northern Hemisphere north of 20N latitude reaches a minimum approximately one day after the passing of a sector boundary, and then increases during the following two or three days. The effect is found at all heights within the troposphere, but is not prominent in the stratosphere, except at the lower levels. No single longitudinal interval appears to dominate the effect.

1. Introduction

A relation between the solar magnetic sector structure and a vorticity area index at 300 mb has recently been reported [Wilcox *et al.* (1973); for recent reviews of related work see Roberts and Olson (1973a) and Svalgaard (1973)]. The solar magnetic sector structure is a large-scale persistent pattern in the sun that has been discovered through spacecraft observations of the interplanetary magnetic field (Wilcox, 1968), and it is a consequence of the solar magnetic field as extended in space by the solar wind. The solar magnetic sector structure is generally known to solar physicists, but is not so well known to meteorologists. We therefore start with a brief description of this structure.

2. The solar magnetic sector structure

Fig. 1 shows spacecraft observations of the polarity (away from or toward the sun) of the interplanetary magnetic field observed near the earth during $2\frac{1}{2}$ solar rotations. The plus (away) and minus (toward) signs at the periphery of the figure represent the field polarity during 3-hr intervals. The four Archimedes spiral lines coming from the sun represent sector boundaries inferred from the spacecraft observations. Within each sector the polarity of the interplanetary field is predominantly in one direction. Since the interplanetary field lines are rooted in the sun, the entire field pattern rotates with the sun with an approximately 27-day period. The solar magnetic sector structure is extended outward from the sun by the radially flowing solar wind. The sector boundaries are often very thin, sometimes approaching a proton gyro radius in thickness. The time at which such boundaries are swept past the earth by the solar wind can therefore often be defined to within a fraction of an hour.

What would a sector boundary shown in Fig. 1 look like on the visible solar disk? Wilcox and Howard (1968) have compared the interplanetary field observed by spacecraft near the earth with the solar photospheric magnetic field deduced from the longitudinal Zeeman effect measured at the 150-ft solar tower telescope at Mount Wilson Observatory. This analysis suggested that an average solar sector boundary is similar to the

[1] The National Center of Atmospheric Research is sponsored by the National Science Foundation.

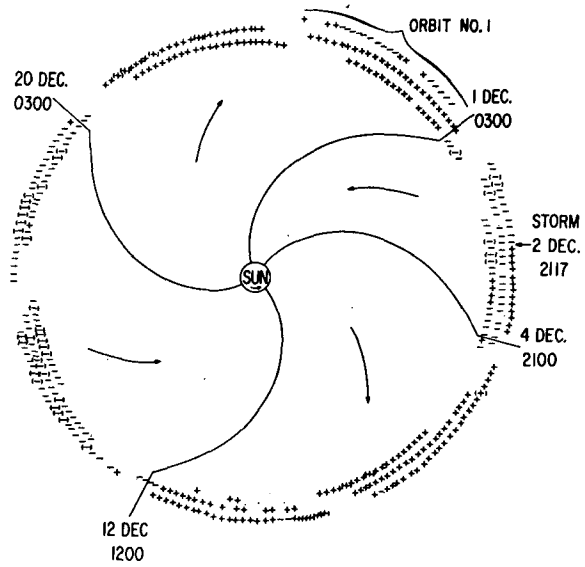

FIG. 1. The inner portion of the figure is a schematic representation of a sector structure of the interplanetary magnetic field that is suggested by observations obtained with the IMP-1 spacecraft in 1963. The plus signs (away from the sun) and minus signs (toward the sun) at the circumference of the figure indicate the direction of the measured interplanetary magnetic field during successive 3-hr intervals. The deviations about the average streaming angle that are actually present are not shown. (After Wilcox and Ness, 1965.)

schematic shown in Fig. 2. The boundary is approximately in the north-south direction over a wide range of latitudes on both sides of the equator. A large area to the right of the boundary has a large-scale field of one polarity and a large-scale region to the left of the boundary has field of the opposite polarity.

Suppose we observe the mean solar magnetic field when the configuration is as shown in Fig. 2. The mean solar magnetic field is defined as the average field of the entire visible solar disk, i.e., the field of the sun observed as though it were a star. In the circumstances shown in Fig. 2, such an observation would yield a field close to zero, since there would tend to be equal and opposite contributions from the left and right sides of the figure.

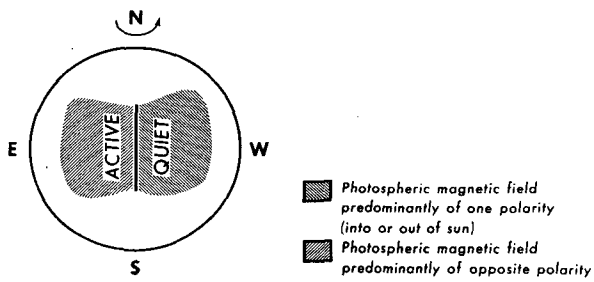

FIG. 2. Schematic of an average solar sector boundary. The boundary is approximately in the north–south direction over a wide range of latitude. The solar region to the west of the boundary is unusually quiet and the region to the east of the boundary is unusually active. (After Wilcox, 1971.)

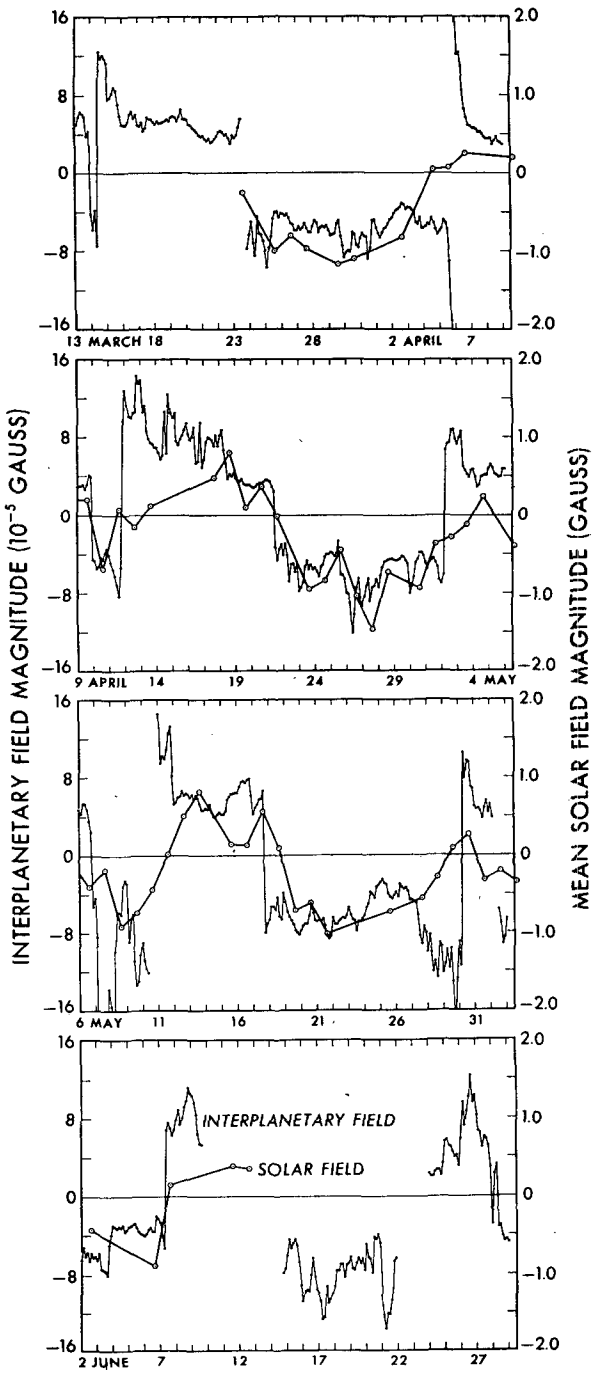

FIG. 3. Comparison of the magnitude of the mean solar field and of the interplanetary field. The open circles are the daily observations of the mean solar field, and the dots 3-hr average values of the interplanetary field magnitude observed near the earth. The solar observations are displaced by $4\frac{1}{2}$ days to allow for the average sun-earth transit time. The abscissa is the time of the interplanetary observations. (After Severny *et al.*, 1970.)

One day later the boundary will have rotated with the sun 13° westward, and the visible disk will be dominated by the sector at the left in Fig. 2. A mean field observa-

tion will now yield a field having the polarity appropriate to the dominant sector. This same polarity will be observed during several subsequent days, until the next sector boundary passes the central meridian and reverses the polarity of the observed mean solar field.

Fig. 3 shows a comparison of the mean solar field observed at the Crimean Astrophysical Observatory with the interplanetary magnetic field observed with spacecraft near the earth (Severny *et al.*, 1970). In this comparison the mean solar field has been displaced by $4\frac{1}{2}$ days to allow for the average transit time from near the sun to the earth of the solar wind plasma that is transporting the solar field lines past the earth. We see in Fig. 3 that in polarity and also to a considerable extent in magnitude the interplanetary field carried past the earth is very similar to the mean solar magnetic field. If we use the observed interplanetary field to investigate effects on the earth's weather, we are using a structure that is clearly of solar origin but is observed at precise times near the earth.

In addition to the sharp, well-defined change of polarity at the boundary, the sector structure has a large-scale pattern. During several days before a boundary is observed to sweep past the earth (or, equivalently, we may say during several tens of degrees of heliographic longitude westward of a boundary), conditions on the sun, in interplanetary space, and in the terrestrial environment tend to be quieter than average. Similarly after the boundary, these conditions tend to be more active than average. A specific example of this is shown in Fig. 4, which shows a superposed epoch analysis of the average effect on the geomagnetic activity index Kp as sector boundaries sweep past the earth. In the days before a boundary, the average geomagnetic activity has a monotonic decline to a minimum about one day before the boundary. Activity then rises to a peak a day or two after the boundary, and then resumes its decline (Wilcox and Colburn, 1972). The Van Allen radiation belts "breathe" inward and outward as the sector structure sweeps past the earth (Rothwell and Greene, 1966). Several other examples of the large-scale geomagnetic response to the sector structure have been given by Wilcox (1968). We emphasize that although the moment at which a sector boundary is carried past the earth provides a well-defined timing signal, the terrestrial effects are related for the most part to the large-scale structure existing for several days on each side of the boundary.

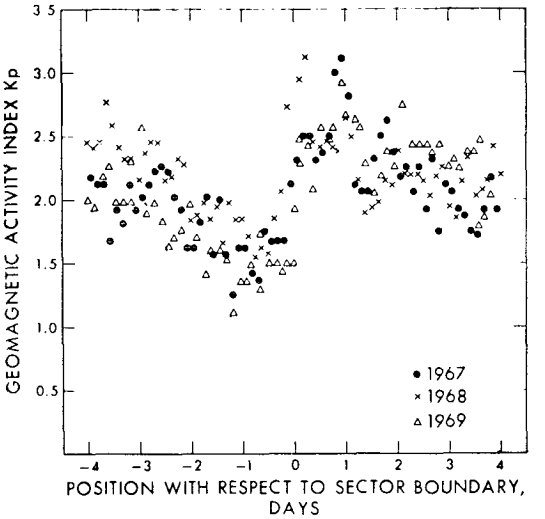

FIG. 4. Superposed epoch analysis of the magnitude of the planetary magnetic 3-hr range indices Kp as a function of position with respect to a sector boundary. The abscissa represents position with respect to a sector boundary, measured in days, as the sector pattern sweeps past the earth. (After Wilcox and Colburn, 1972.)

3. Advantages of solar magnetic sector structure for investigations of effects on weather

From the above discussion, it appears reasonable to use the solar magnetic sector structure in an investigation of possible effects on the earth's weather. The use of the sector structure for this purpose has several advantages. We are using a fundamental large-scale property of the sun. There can then be no doubt that any observed atmospheric response to the passing of a sector boundary is ultimately caused by the solar magnetic sector structure. We emphasize that "solar magnetic sector structure" is a name for the *entire* structure discussed above. When we say that an atmospheric response is caused by the solar magnetic sector structure, we include possibilities that the effect has been transmitted through interplanetary space in the form of magnetic fields, solar wind plasma, energetic particles, or radiation. Similarly, an atmospheric effect observed in the troposphere may flow through the higher atmospheric layers in an exceedingly complex manner. We discuss in this paper only the start (the solar magnetic sector structure) and the result (an effect in the troposphere) of what may be an exceedingly complex flow of physical processes.

We discuss some further advantages of the sector structure for this investigation. In the sense discussed above, a tropospheric response does not have its ultimate cause in other atmospheric processes. Some earlier investigations of solar activity and the weather have been criticized in this respect by Hines (1973). Because of the 4 or 5 day transit time of the solar wind plasma from the sun to the earth, we can have, by observing the mean solar magnetic field, a 4 or 5 day forecast of the time at which a sector boundary will sweep past the earth. By improving the solar observation procedure, we may be enabled to detect a sector boundary 2 or 3 days after it has rotated past the eastern limb of the sun. This would add an additional 4 or 5 days to the forecast interval.

From one solar rotation to the next, the sector structure usually does not change very much. In the

TABLE 1. Observed and well-defined sector boundaries used in the present investigation. The date, sign change (+ away, − toward), and time (in 3-hr intervals) is given for all observed sector boundaries with at least 4 days of opposite field polarity on each side of the boundary. The notation 8–1 means that the boundary occurred between the last 3-hr interval of that day and the first 3-hr interval of the next day.

Year	Day of year	Sign	Date	Time
1964	007	+, −	January 7	7–8
	016	−, +	January 16	2–2 (gap)
	023	+, −	January 23	3–4
	035	+, −	February 4	2–3
	306	+, −	November 1	5–6
	312	−, +	November 7	2–1 (gap)
	320	+, −	November 15	5–6
	325	−, +	November 20	3–2 (gap)
	332	+, −	November 27	7–8
	341	−, +	December 6	4–5
	345	+, −	December 10	8–1
	349	−, +	December 14	8–1
	361	+, −	December 26	1–2
1965	002	−, +	January 2	1–2
	008	+, −	January 8	1–2
	012	−, +	January 12	2–3
	032	+, −	February 1	8–1
1966	001	+, −	January 1	6–7 (1 day gap)
	032	+, −	February 1	4–5
	043	−, +	February 12	2–3
	062	+, −	March 3	3–4
	067	−, +	March 8	2–3
	089	+, −	March 30	2–3
	312	+, −	November 8	4–5
	331	−, +	November 27	7–8
	338	+, −	December 4	3–4
1967	001	+, −	January 1	7–8
	013	+, −	January 13	3–4
	018	−, +	January 18	2–3 (1 day gap)
	081	−, +	March 22	7–8
	324	−, +	November 20	4–5
	338	+, −	December 4	5–6
1968	001	+, −	January 1	6–5 (gap)
	028	+, −	January 28	8–1
	042	−, +	February 11	3–4
	057	+, −	February 26	6–7
	070	−, +	March 10	4–5
	083	+, −	March 23	5–6
	318	+, −	November 13	2–3
	334	−, +	November 29	6–8 (gap)
	345	+, −	December 10	2–3
	359	−, +	December 24	6–7
1969	006	+, −	January 6	5–6
	023	−, +	January 23	8–1
	033	+, −	February 2	5–6
	050	−, +	February 19	2–3
	090	+, −	March 31	6–7
	330	−, +	November 26	5–6
	343	+, −	December 9	1–2
	356	−, +	December 22	7–8
1970	040	−, +	February 9	7–8
	067	−, +	March 8	8–1
	309	−, +	November 5	3–4
	328	+, −	November 24	3–4

course of a year there are often significant changes in the sector structure, which appears to have significant variations through the 11-year sunspot cycle (Svalgaard, 1972). All of these regularities and recurrence properties may be of significant assistance in forecasting. As the solar magnetic sector structure and its interplanetary and terrestrial consequences become better understood in the coming years, the possibilities of using solar data in weather forecasting should also improve.

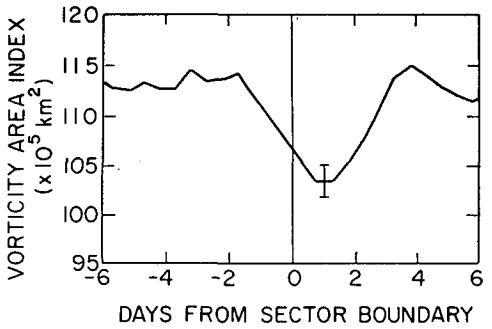

FIG. 5. Average response of the vorticity area index to the solar magnetic sector structure during the winter period. Sector boundaries were carried past the earth by the solar wind on day zero.

4. Response of vorticity area to sector structure

In the present investigation the method of superposed epochs is used to give the average response of a vorticity area index to the passage of 54 sector boundaries. These boundaries, which are listed in Table 1, were observed with spacecraft near the earth from 1964 through 1970 during the winter months November through March (the effects described below did not appear during the summer months). These boundaries were observed to have one predominant polarity of the interplanetary magnetic field for at least 4 days before the boundary, and the other polarity of the interplanetary magnetic field during at least 4 days after the boundary. A list of well-defined sector boundaries was published by Wilcox and Colburn (1972) before we began the present investigation. To this we have added boundaries for the year 1970.

The vorticity area index was devised by Roberts and Olson (1973b). Pressure height maps at 0000 and 1200 GMT for each day are used to compute vorticity maps at the 300-mb level of the atmosphere. Prominent features of such vorticity maps are the regions of high vorticity, and these coincide closely with the low pressure troughs visible on contour maps of the heights of given pressure surfaces at the same level. The region of the Northern Hemisphere north of 20N is shown on these maps. A "discriminator" of 20×10^{-5} sec^{-1} is applied to a vorticity map, and the area (km^2) in which the vorticity exceeds this value is recorded. The discriminator is then set at 24×10^{-5} sec^{-1} and the area in which the vorticity exceeds this value is added to the previously computed area. (In some of the investigations reported in the present paper, we have used a single discriminator setting, usually 20×10^{-5} sec^{-1}. In

the vorticity area index of Roberts and Olson, the discriminator setting at 24×10^{-5} sec^{-1} usually contributed about 15% to the total index, so that a single discriminator setting of 20×10^{-5} sec^{-1} gives results that are very similar to those obtained with the vorticity area index.)

The average response of the vorticity area index to the 54 well-defined sector boundary crossings described above is shown in the superposed epoch analysis of Fig. 5. The vorticity area index reaches a minimum approximately 1 day after the boundary, and then increases during the next 2 or 3 days. At the 300-mb height shown in Fig. 5 the amplitude of the effect is about 10%. (In order to remove variations apparently caused by the differences in analysis between 0000 and 1200, the vorticity area index V was smoothed according to the formula $V_i=(\frac{1}{2}V_{i-1}+V_i+\frac{1}{2}V_{i+1})/2$, where the V_i are successive values at 12-hr intervals.)

It is clearly important to establish the physical and statistical significance of the influence of the solar magnetic sector structure on tropospheric vorticity shown in Fig. 5, because if the reality of this influence becomes generally accepted then the task of understanding the physical processes will attract more attention and have better chance of success.

We have computed the standard error of the mean of the 54 values of the vorticity area index corresponding to Day 1 in Fig. 5 in the following manner. We are interested in variations in the index in the interval a few days before and after the passing of a sector boundary. Longer term variations in the index such as seasonal effects should not be included in the calculation of the standard error. Therefore, for each sector boundary we compute the average value of the vorticity area index during the interval ±6 days from that boundary, and from this we subtract the grand average of the vorticity area index during all days in the intervals ±6 days from the 54 sector boundaries. Call

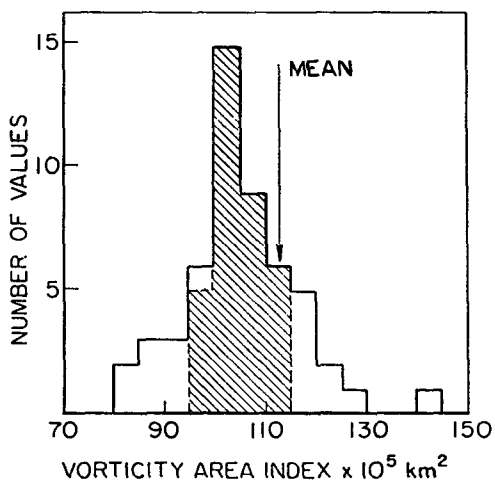

FIG. 6. Distribution of values of vorticity area index for time equal to 1 day after a sector boundary passes the earth.

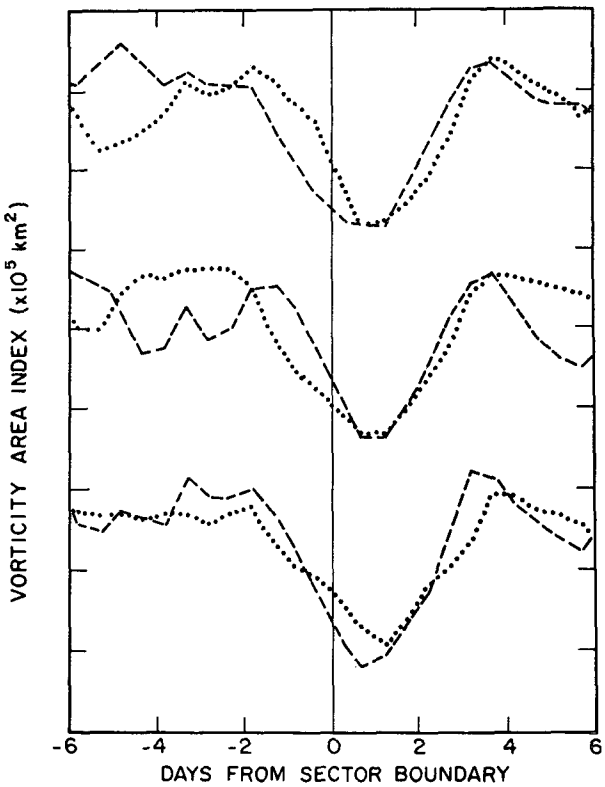

FIG. 7. As in Fig. 5 except that the list of boundaries used in Fig. 5 has been divided into three two-part groupings: 1) the magnetic polarity change at the boundary, 2) the first or last half of winter, and 3) the yearly intervals 1964–66 and 1967–70.

1) The dotted curve represents 24 boundaries in which the interplanetary magnetic field polarity changed from toward the sun to away, and the dashed curve 30 boundaries in which the polarity changed from away to toward.
2) The dotted curve represents 32 boundaries in the interval 1 November to 15 January, and the dashed curve 22 boundaries in the interval 16 January to 31 March.
3) The dotted curve represents 26 boundaries in the interval 1964 to 1966, and the dashed curve 28 boundaries in the interval 1967 to 1970.

The curves have been arbitrarily displaced in the vertical direction, but the scale of the ordinate is the same as in Fig. 5, i.e., each interval is 5×10^5 km².

the result of this subtraction for each sector boundary Δ_j, where j runs from 1 to 54. Fig. 6 shows the distribution of the 54 values $V_j-\Delta_j$, where V_j is the value of the vorticity area index one day after the passing of the jth sector boundary. The average value of the index during all intervals ±6 days from the 54 sector boundaries is also shown in Fig. 6. Since 65% of the values in Fig. 6 (see cross-hatched area) lie in the range $(104\pm12)\times10^5$ km², the probable error of the mean is of the order $(12/\sqrt{53}=1.6)\times10^5$ km², and this is the error bar shown in Fig. 5.

The significance and reproducibility of the effect has been further investigated by dividing the list of 54

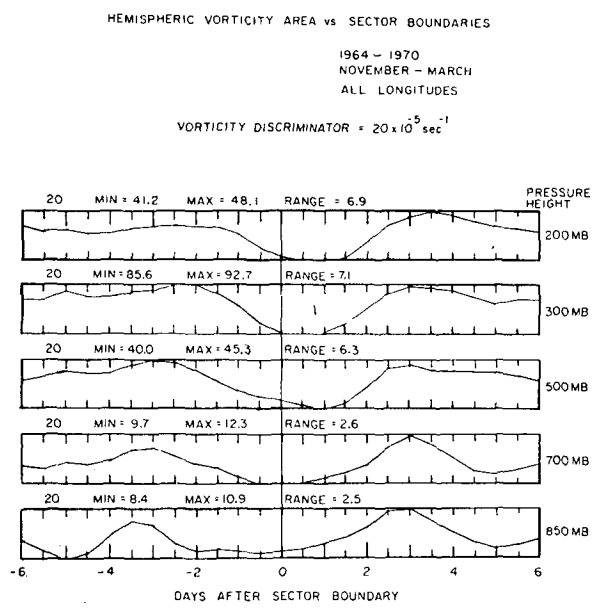

FIG. 8. Superposed epoch analyses of average response of hemispheric vorticity area to the passing of 54 sector boundaries in the interval November through March of 1964 through 1970. Areas in the Northern Hemisphere north of 20N in which the vorticity exceeded a value of 20×10^{-5} sec^{-1} are included. The results are shown for pressure levels of 200, 300, 500, 700 and 850 mb. Each graph includes the maximum and minimum values of the vorticity area within range ±6 days from the sector boundary. At the top of each graph is listed the vorticity discriminator in units of 10^{-5} sec^{-1}, and the minimum, maximum and range of the vorticity area in units of 10^5 km^2.

sector boundaries into two parts, and performing the same superposed epoch on each part separately. The results are shown in Fig. 7, in which the list of boundaries was divided into three two-part groupings: 1) the magnetic polarity change at the boundary, 2) the first or last half of winter, and 3) the yearly intervals 1964–66 and 1967–70. We see in Fig. 7 that the effect persists with little change when the data set is divided into two parts in these various ways. The results shown in Figs. 5 and 7 indicate that further attention should be given to investigations of the physical processes involved in the influence of the solar magnetic sector structure on the earth's weather.

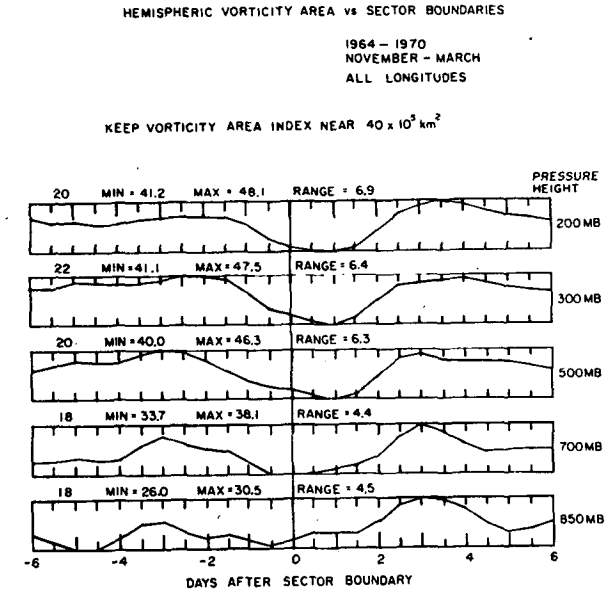

FIG. 9. As in Fig. 8 except that the vorticity discriminator is adjusted so as to keep the vorticity area near a value of 40×10^5 km^2.

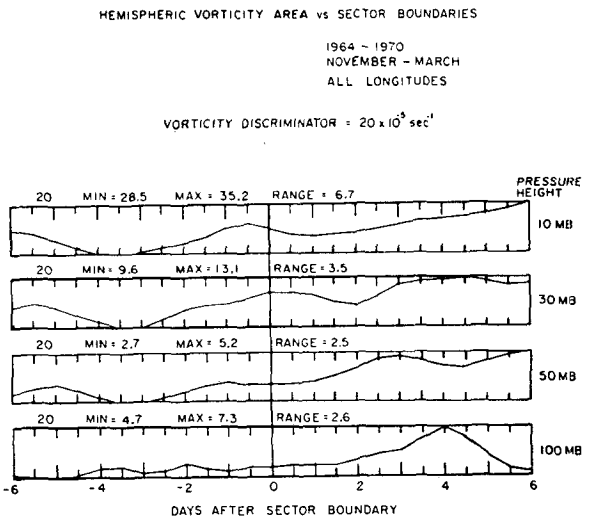

FIG. 10. As in Fig. 8 except that pressure levels in the stratosphere are shown. The effect found in Fig. 8 in the troposphere is not prominent in the stratosphere.

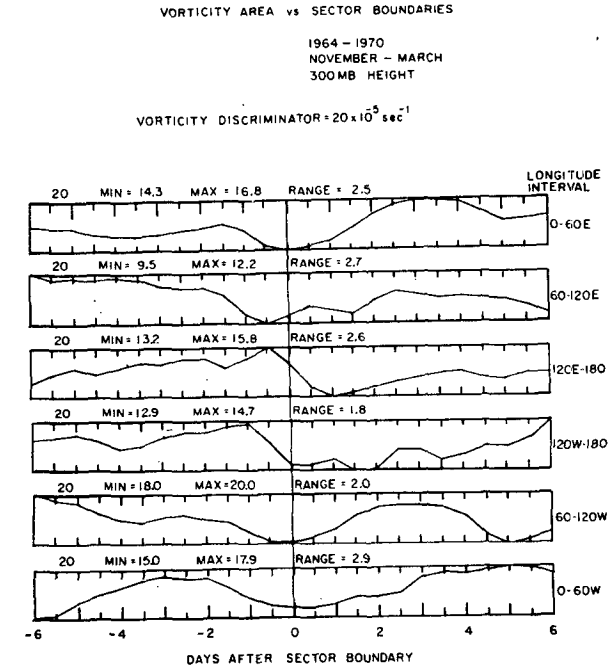

FIG. 11. As in Fig. 8 except at a pressure level of 300 mb. Results for longitude intervals 60° wide are shown. No single interval dominates the observed effect.

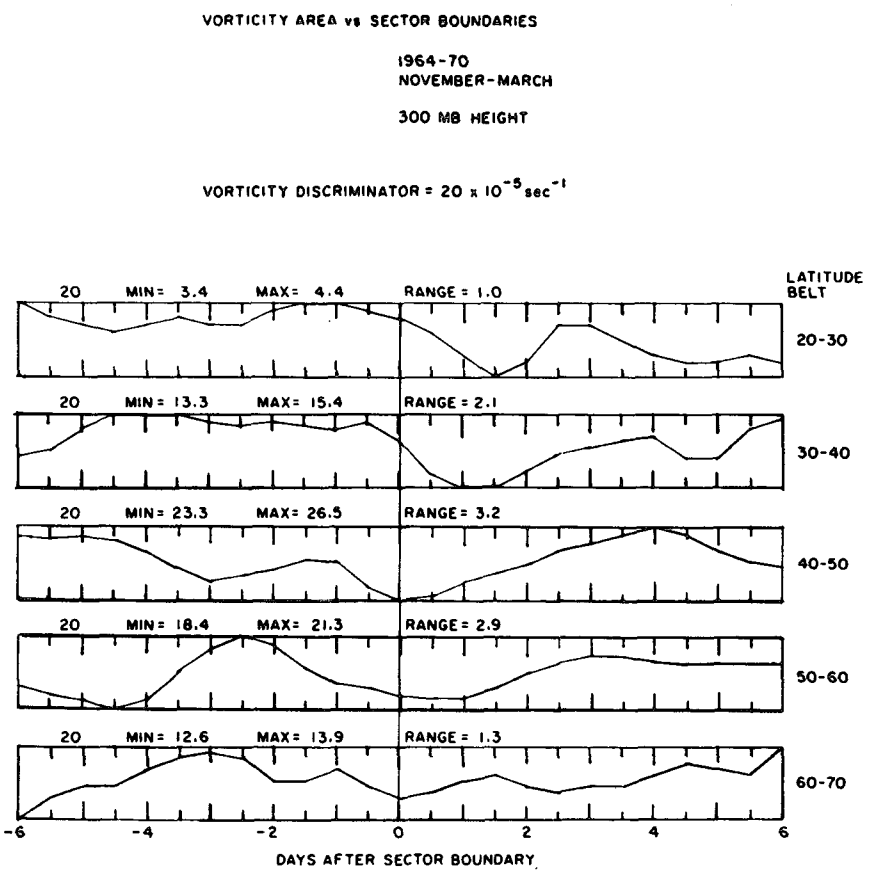

FIG. 12. As on Fig. 8 except that results are shown in latitude belts 10° wide in the interval from 20N to 70N. The results are shown for a pressure level of 300 mb.

The above results were all studied at the 300-mb level; we proceed now to investigate the effect at other heights in the troposphere. Fig. 8 shows the results of a superposed epoch analysis similar to that used in preparing Fig. 5 at pressure levels of 200, 300, 500, 700 and 850 mb. The format for Fig. 8 and the following figures is that above each superposed epoch curve is given a number that represents the vorticity discriminator in units of 10^{-5} sec^{-1}, and the minimum, maximum and range of the vorticity area in units of 10^5 km^2. In Fig. 8 we have set the vorticity discriminator at 20, and the resulting values of vorticity area are less than those shown in Fig. 5, which had an additional contribution from a discriminator setting of 24. However, if we compare the graph in Fig. 8 for 300 mb with Fig. 5 which is at the same height, we see that the effect is very similar. In Fig. 8 we see an ordered response of the vorticity area to the passing of a sector boundary at all heights within the troposphere. As we go from the top of the troposphere (or the lowest levels of the stratosphere) down to ground level, the width of the minimum near the boundary increases considerably. An increase from about 1 day after the boundary to 3 days after the boundary is a persistent feature of the response at all heights in the troposphere.

We now examine a somewhat technical point in the analysis. We note in Fig. 8 that when we hold the vorticity discriminator constant at 20, we find that the resulting areas change by a considerable factor over the range of heights investigated. Another method of analysis could be to adjust the vorticity discriminator such as to keep the area approximately constant, near a value such as 40×10^5 km^2. This approach has been followed in preparing Fig. 9, which is otherwise similar to Fig. 8. The graphs in the two figures are very similar, showing that the response is essentially the same for these two methods of investigation.

We next investigate the response of the vorticity area in the stratosphere. The result is shown in Fig. 10, which is similar in format to Fig. 8. We see that the effect discussed above in the troposphere is not prominent in the stratosphere, though at 100 mb the peak at 4 days after the boundary is evident and probably significant.

All the above discussion has included the vorticity area obtained in the entire Northern Hemisphere north of 20N. We wish to investigate whether a particular longitudinal interval in this hemisphere has a predominant influence on the observed effect. For this purpose the hemisphere was divided into intervals of

60° in longitude, and the same superposed epoch analysis was performed for each such interval with the results shown in Fig. 11, which is similar in format to Fig. 8. The graphs in Fig. 11, however, are considerably noisier than those in Fig. 8 largely because each longitudinal interval shown in Fig. 11 will tend to have only one or two low pressure troughs contained within it. There are usually ten or twelve low pressure troughs distributed around the Northern Hemisphere. Thus, in Fig. 11 the amount of area that goes into the superposed epoch averaging process is decreased by about an order of magnitude, and the noise in the resulting graphs is thereby increased. After seeing Fig. 11, we again verified that if these six superposed epoch curves are combined into one curve the much smoother graph shown in Fig. 8 indeed results. Each of the longitude intervals shown in Fig. 11 has a minimum near the passing of the sector boundary. The ranges shown for each longitudinal interval vary only in the limited interval from 1.8 to 2.9, so it is clear that the global effect shown in Fig. 8 does not result from only one or two prominent longitudinal intervals.

The cleaner response shown for a hemispheric investigation in Fig. 8 compared with the noisier results obtained for individual longitudinal sectors in Fig. 11 is reminiscent of a similar situation encountered when observing the magnetic sector structure on the sun. When the field of the entire visible disk of the sun is averaged in the observation, a clear sector pattern is observed for each individual sector (as shown in Fig. 3). If, on the other hand, only a limited area of the sun is observed, then the structure of individual sectors is less clear and statistical techniques involving observations of several sectors usually must be employed (Wilcox, 1968).

The same superposed epoch analysis has been performed in 10° latitude belts in the interval 20–70N with the results shown in Fig. 12. The graphs again are noisier than was the case in Fig. 8 for reasons similar to those just discussed. Each latitude belt displays a minimum near the passing of the sector boundary. The principal contribution to the hemispheric vorticity area effect comes from the middle latitudes, which is also where the largest vorticity regions are located.

5. Summary

It appears that the solar magnetic sector structure has a definite influence on the earth's weather during the winter period. At all heights in the troposphere and in the lowest part of the stratosphere, the vorticity area is a minimum near the passing of the sector boundary and increases during 2 or 3 days thereafter. This effect is not prominent in the stratosphere, except at the very lowest levels. The effect does not appear to be predominent in only one or two longitudinal intervals. The chief contribution to the global effect comes from mid-latitudes.

In our opinion the chief purpose of a statistical investigation such as that reported here is to point the way toward specific investigations directed toward understanding the physical processes involved in the influence of the solar sector structure upon the earth's weather. We look forward to pursuing such investigations.

Acknowledgments. This work was supported in part by the Office of Naval Research under Contract N00014-67-A-0112-0068, by the National Aeronautics and Space Administration under Grant NGR 05-020-559, and by the Atmospheric Sciences Section of the National Science Foundation under Grant GA-31138. The work was also supported in part by the National Center for Atmospheric Research, which is sponsored by the National Science Foundation.

REFERENCES

Hines, C. O., 1973: Comments on "A test of an apparent response of the lower atmosphere to solar corpuscular radiation." *J. Atmos. Sci.*, **30**, 739–744.

Roberts, W. O., and R. H. Olson, 1973a: New evidence for effects of variable solar corpuscular emission upon the weather. *Rev. Geophys. Space Phys.*, **11**, 731–740.

——, and ——, 1973b: Geomagnetic storms and wintertime 300-mb trough development in the North Pacific–North Atlantic area. *J. Atmos. Sci.*, **30**, 135–140.

Rothwell, P., and C. Greene, 1966: Spatial and temporal distribution of energetic electrons in the outer radiation belt. Report, University of Southhampton.

Severny, A., J. M. Wilcox, P. H. Scherrer and D. S. Colburn, 1970: Comparison of the mean photospheric magnetic field and the interplanetary magnetic field. *Solar Phys.*, **15**, 3–14.

Svalgaard, L., 1972: Interplanetary magnetic-sector structure, 1926–1971. *J. Geophys. Res.*, **77**, 4027–4034.

——, 1973: Solar activity and the weather. *Proceedings Seventh ESLAB Symposium*, Reidel, Dordrecht, Holland (to be published).

Wilcox, J. M., 1968: The interplanetary magnetic field. Solar origin and terrestrial effects. *Space Sci. Rev.*, **8**, 258–328.

——, 1971: Solar sector magnetism. *Comments Astrophys. Space Phys.*, **3**, 133–139.

——, and D. S. Colburn, 1972: Interplanetary sector structure at solar maximum. *J. Geophys. Res.*, **77**, 751–756.

——, and R. Howard, 1968: A large-scale pattern in the solar magnetic field. *Solar Phys.*, **5**, 564–574.

——, and N. F. Ness, 1965: Quasi-stationary corotating structure in the interplanetary medium. *J. Geophys. Res.*, **70**, 5793–5805.

——, P. H. Scherrer, L. Svalgaard, W. O. Roberts and R. H. Olson, 1973: Solar magnetic sector structure: Relation to circulation of the earth's atmosphere. *Science*, **180**, 185–186.